

Water induced Restructuring of Vanadia clusters supported on α -TiO₂ (101) hydration dynamics

(Dated: 9 March 2020)

I. INTRODUCTION

II. EXPERIMENTAL CLAIM

After the deposition of vanadium oxide clusters on clean anatase-TiO₂ (101) surface, they exposed to water. In the same experiment they de-exposed the water and captured the STM images at all instances of partial water vapour pressure (P_{O_2}) conditions. The final STM images were shown in Fig. 1 (a), vanadium oxide clusters on clean surface, Fig 1(b)- vanadium oxide clusters after reaction with water and Fig. 1(c)- vanadium oxide clusters when they de-expose water after the reaction happens.

In Fig 1(a), only one feature observed and in Fig 1(b) and 1(c) there are two distinct features were observed. The observations from STM images from Fig 1(a) - Fig 1(b), indicates that there is restructuring of these vanadium clusters due to reaction between water and vanadium oxide clusters. The STM image (Fig 1(c)) during de-exposure, indicating that there is reshaping of vanadium oxide clusters after reaction with water. And interestingly they achieved the reversibility between Fig 1(c) to Fig 1(b) and vice-versa. This gives an evidence that due to water reaction with vanadium oxide clusters, they were not observed same features as on clean surface.

III. FUNDAMENTAL QUESTIONS RAISED FROM THEORY

i) There is no clear evidence that what is the molecular form of these features *ii)* Why same features were not observed after and during water exposure *iii)* No clear evidence of what is the composition of oxygen while formation of oxide clusters

IV. METHODOLOGY

In order to answer for the key questions raised in previous section, we have considered monomer and dimer vanadium oxide clusters to explore different oxidation states of Vanadium such as VO₂, V₂O₄ and V₂O₅. Thereafter we added one water and two water molecules to these oxides individually and ran unbiased global optimisations. In the present work, we have used anatase-TiO₂ (101) surface with three layer. Top two layers are allowed for relaxations and bottom layer was frozen. Different sized super cells as shown in Fig 2 are used in this work. Very small clusters (VO₂) are done on the 2 × 1 and medium sized clusters (VO₂H₂O, VO₂2H₂O, V₂O₄

and V₂O₄H₂O and V₂O₄2H₂O) are done on the 3 × 1 super cell and bigger clusters are done on the 4 × 1 super cell. All the global optimization runs were done on the stoichiometric surface with respective super cell sizes mentioned here based on the different size of the cluster. After global optimizations low-lying isomers are collected based on the DFT energy. Further, we have re-optimized these structures with reduced surface by creating one oxygen vacancy in second layer. The final order of the structures are considered based on the DFT energy with reduced surface, because in the experiments the surface is reduced.

In this work, global optimization of first principle energy evaluation(GOFEE) was used as global optimization method. It explores the potential energy surface and simultaneously it constructs the machine learning surrogate potential energy and using this potential it finds global minimum.

V. RESULTS

A. low-lying isomers found for VO₂ , VO₂H₂O and VO₂2H₂O clusters

B. low-lying isomers found for V₂O₄ , V₂O₄H₂O and V₂O₄2H₂O clusters

C. low-lying isomers found for V₂O₅ , V₂O₅H₂O and V₂O₅2H₂O clusters

D. Binding Energies for V₂O₅ , V₂O₅H₂O and V₂O₅2H₂O clusters

VI. NEB CALCULATION ON 4 × 1 CELL FOR VO₃H DIFFUSION

VII. REFERENCES

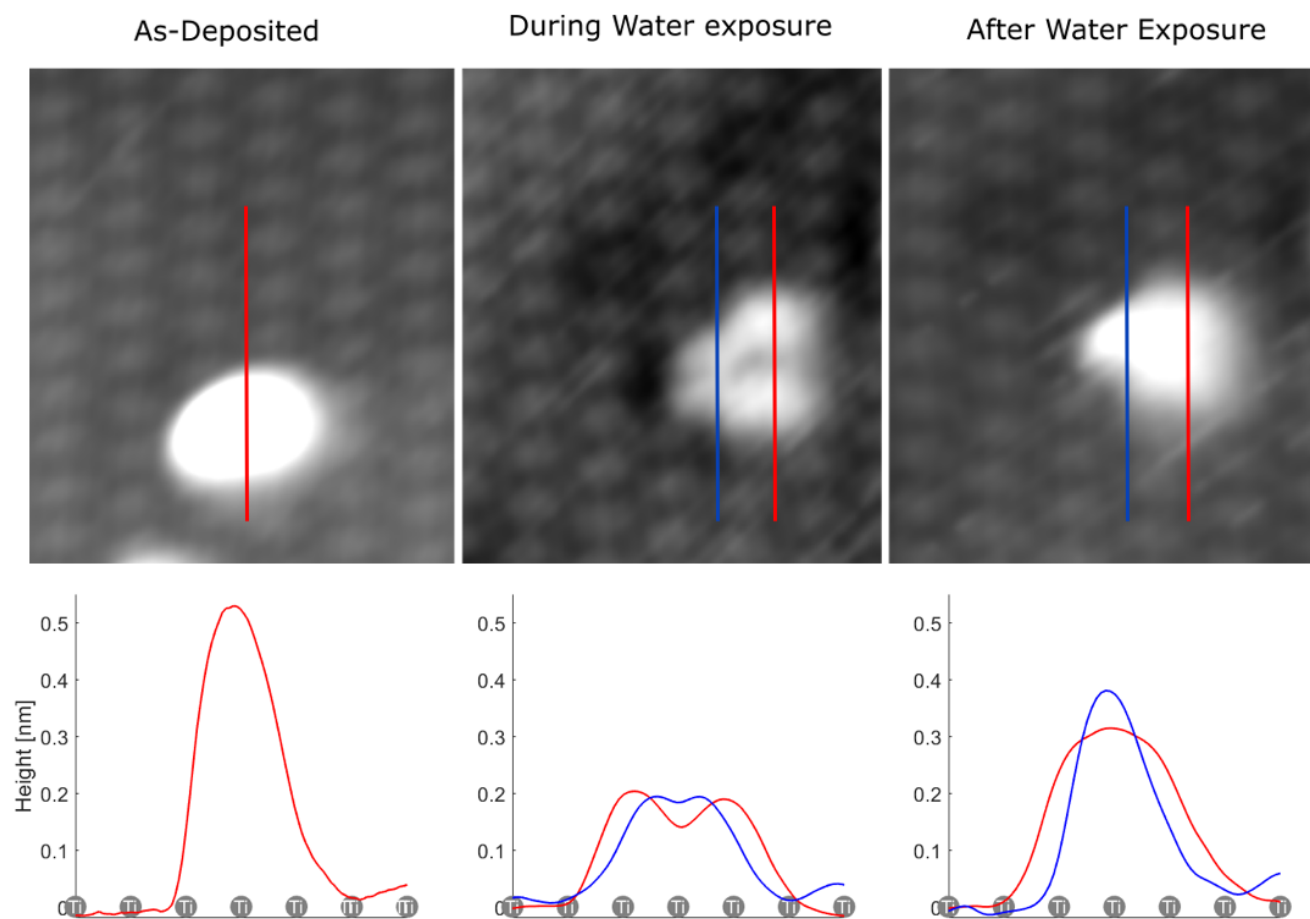


FIG. 1. Experimental Observation

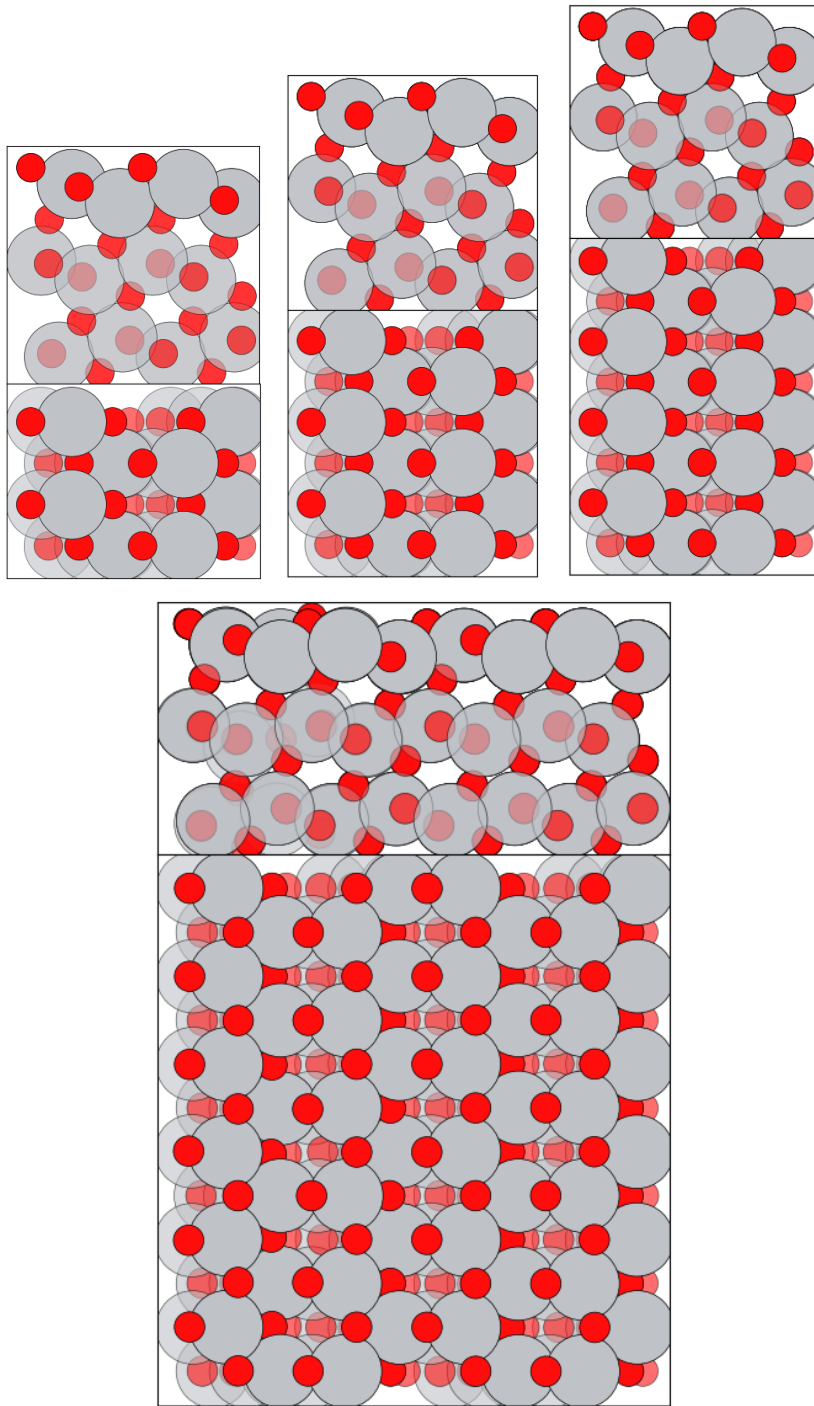


FIG. 2. Different super cell size of surfaces used in all the calculations.

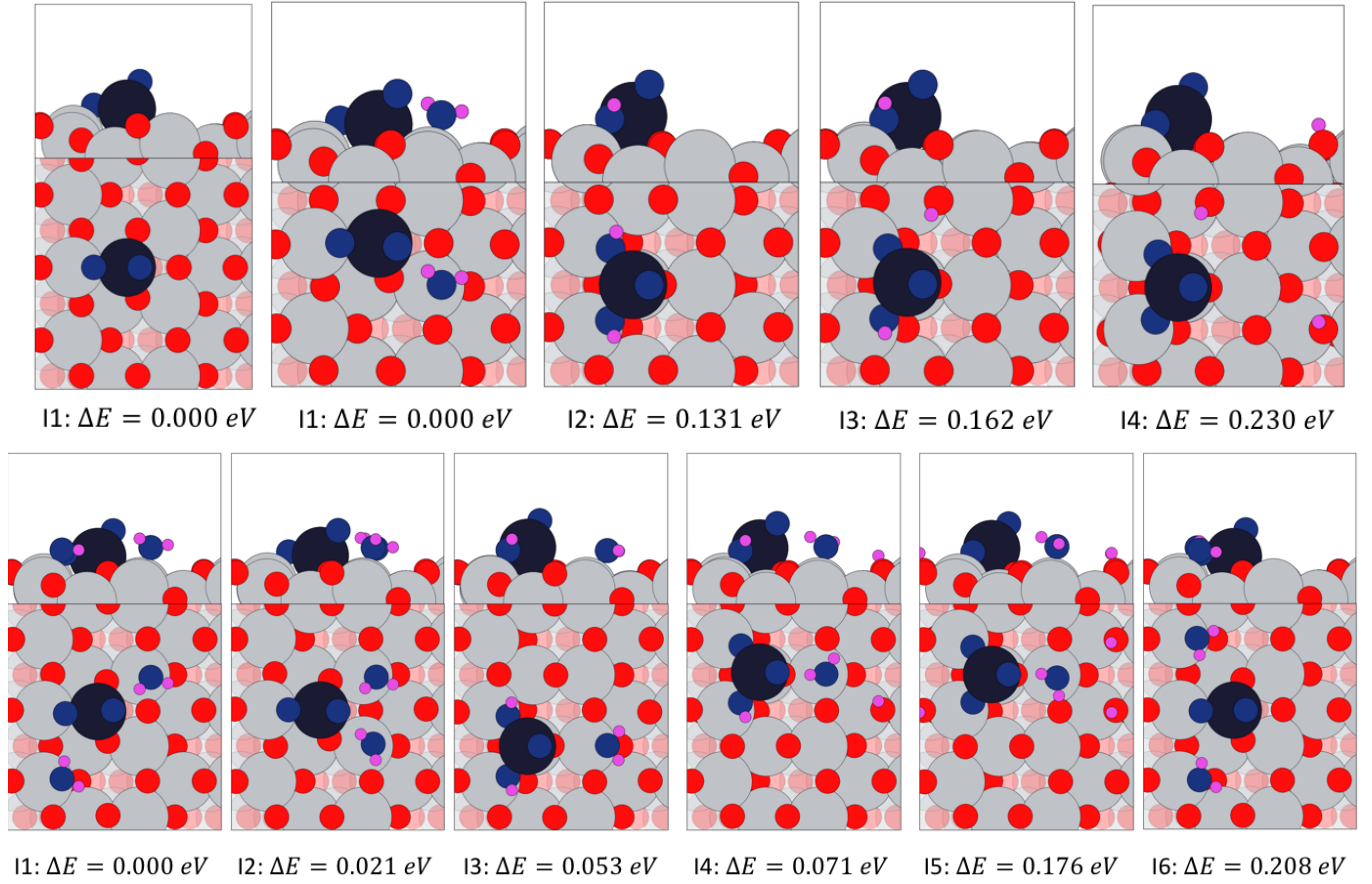


FIG. 3. All the possible low-lying isomers found for VO_2 , $\text{VO}_2\text{H}_2\text{O}$ and $\text{VO}_22\text{H}_2\text{O}$ clusters with GOFEE were DFT relaxed with one Oxygen vacancy created in 2nd layer. Here two types of super cell sizes were used those are $2 \times 1 \times 1$ super cell for VO_2 , $\text{VO}_2\text{H}_2\text{O}$ and $3 \times 1 \times 1$ super cell for $\text{VO}_22\text{H}_2\text{O}$ clusters.

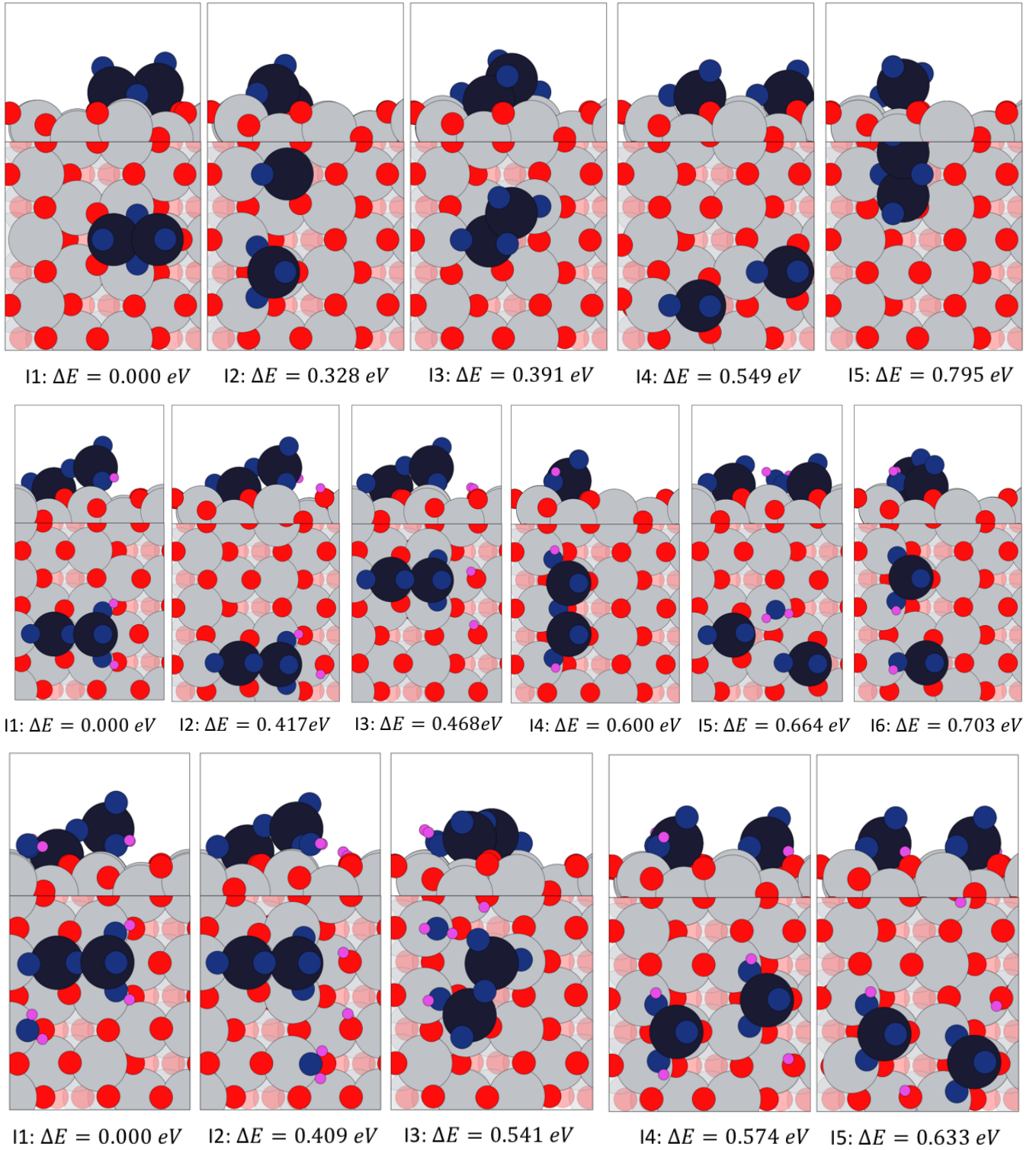


FIG. 4. All the possible low-lying isomers found for V_2O_4 , $\text{V}_2\text{O}_4 \cdot \text{H}_2\text{O}$ and $\text{V}_2\text{O}_4 \cdot 2\text{H}_2\text{O}$ clusters with GOFEE were DFT relaxed with one Oxygen vacancy created in 2nd layer. Here $3 \times 1 \times 1$ super cell used for all clusters.

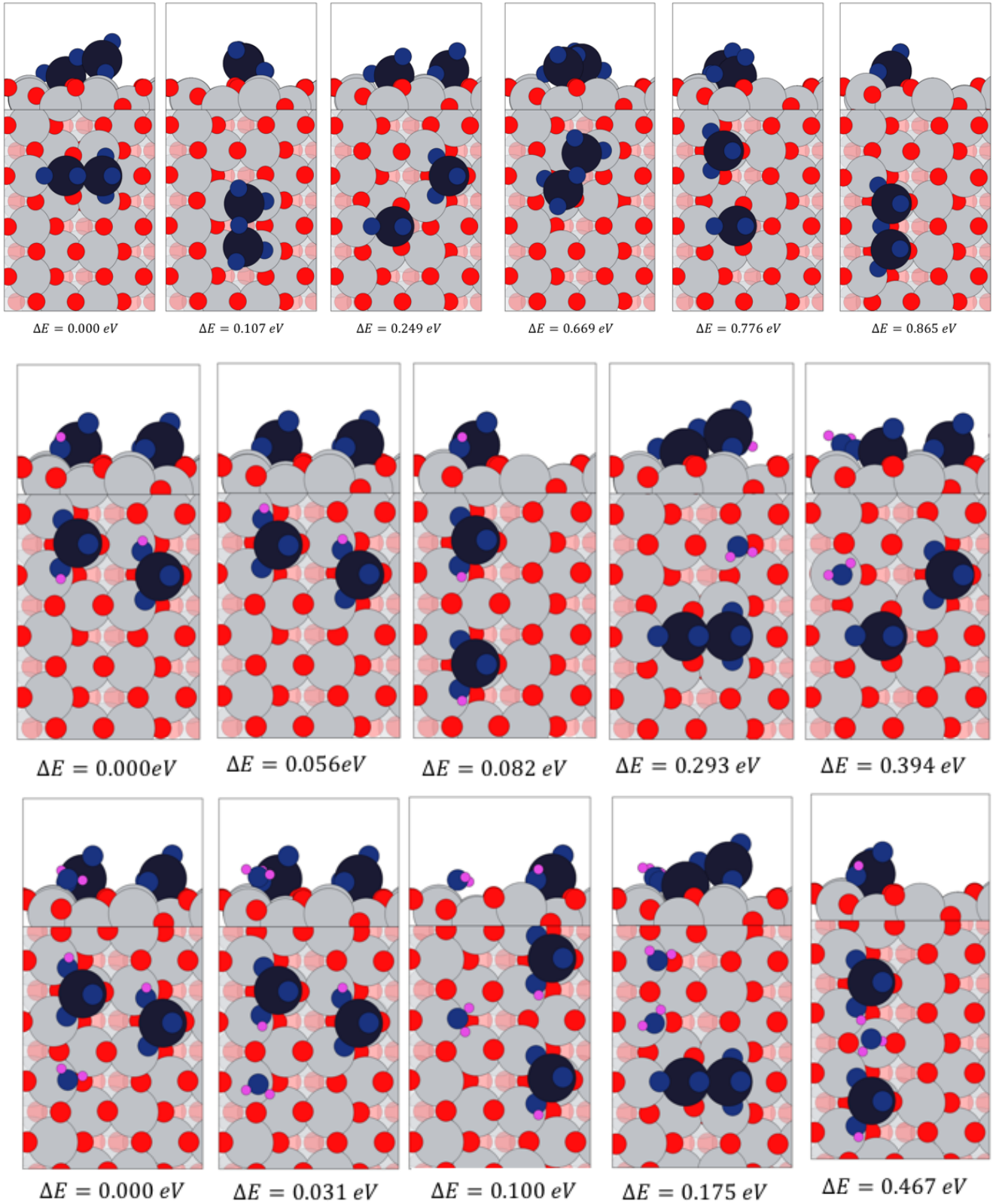


FIG. 5. All the possible low-lying isomers found for V_2O_5 , $V_2O_5H_2O$ and $V_2O_52H_2O$ clusters with GOFEE were DFT relaxed with one Oxygen vacancy created in 2nd layer. Here $4 \times 1 \times 1$ super cell used for all clusters.

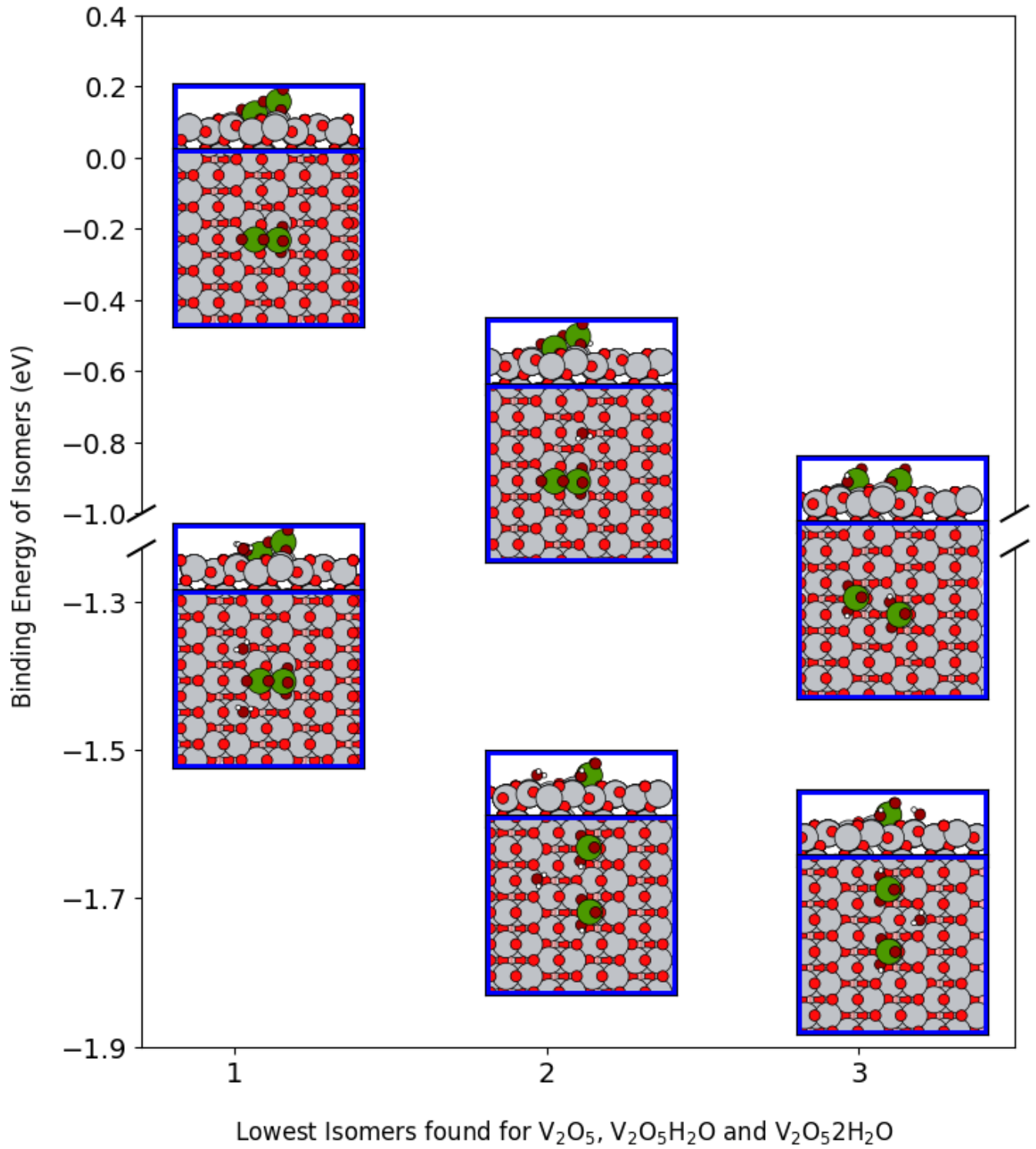


FIG. 6. Binding energy order for best structures of V_2O_5 , $V_2O_5 H_2O$ and $V_2O_5 2H_2O$ clusters found in global optimization were re-optimised with $6 \times 2 \times 1$ super cell and one oxygen vacancy created.

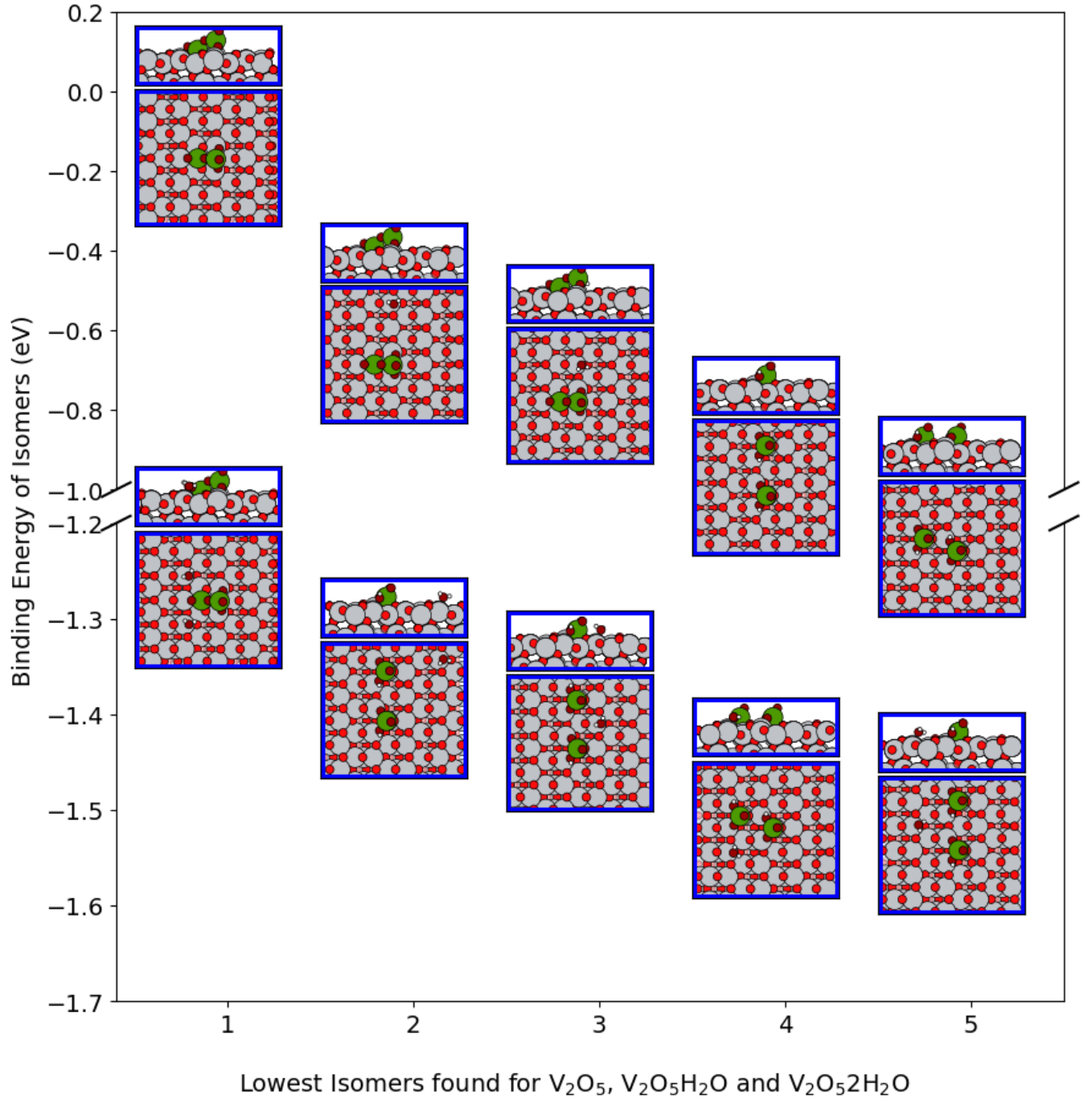


FIG. 7. Binding energy order for best structures of V_2O_5 , $V_2O_5H_2O$ and $V_2O_52H_2O$ clusters found in global optimization were re-optimised with $6 \times 2 \times 1$ super cell and two oxygen vacancy created.

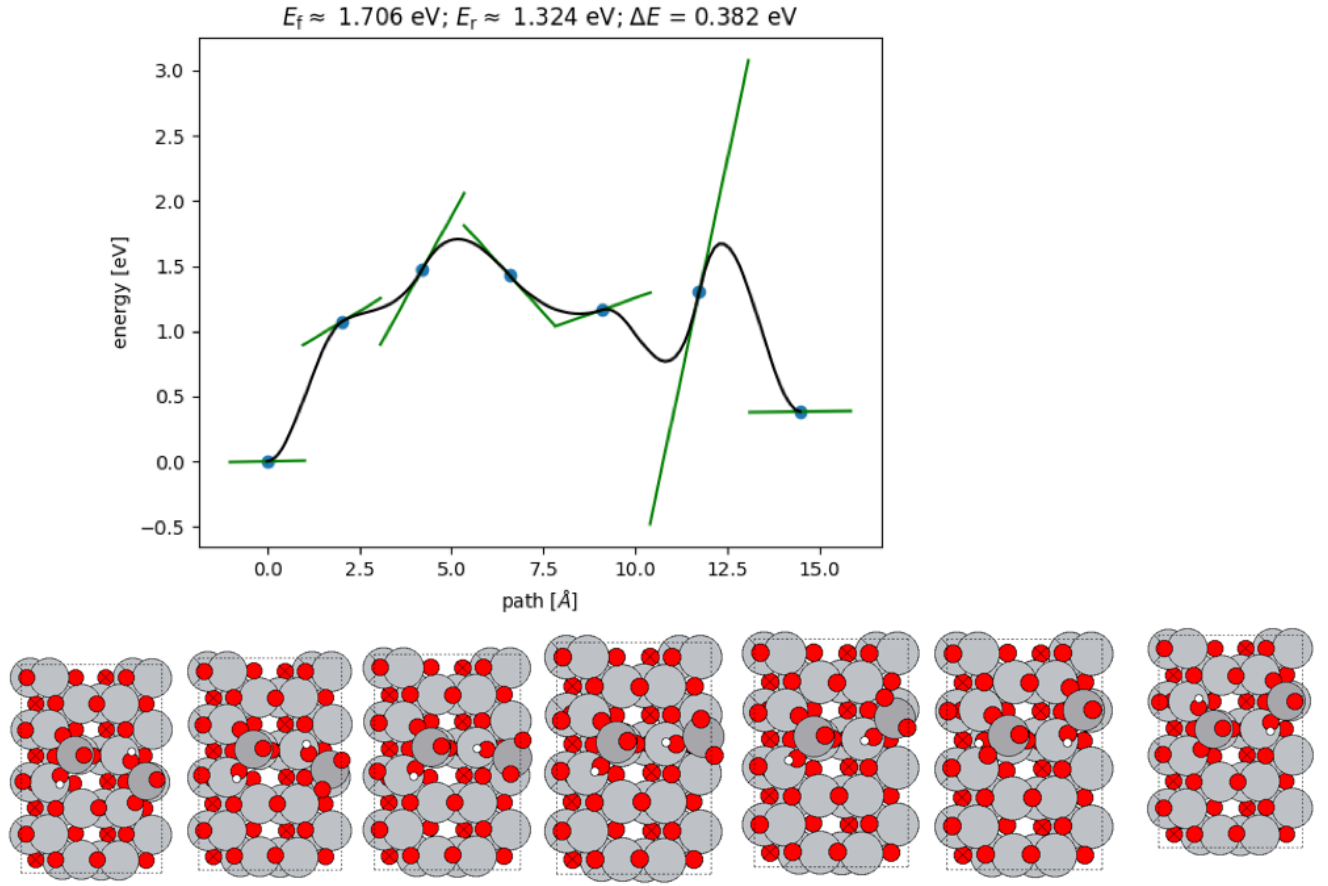


FIG. 8. NEB calculations